VNU Journal of Science: Mathematics - Physics

Journal homepage: https://js.vnu.edu.vn/MaP

Original Article

Influence of Calcium on the Structure and Hydrophilic of $CaTiO_3$ Coating on Titanium Implants

Nguyen Thi Thanh Tuyen[1], Nguyen Duc Trung Kien[2], Nguyen Xuan Viet[1], Lo Thi Thuy Linh [1], Tran Thi Ngoc Huyen[1], Nguyen Thi Mai Anh[1], Nguyen Van Lam[1], Truong Quoc Phong[1], Mai Xuan Dung[3], Dao Hong Bach[1], Dang Nhat Minh[4], James Wang[4], Pham Hung Vuong[1,*]

[1]*Hanoi University of Science and Technology (HUST), 1 Dai Co Viet, Hanoi, Vietnam*

[2]*Phenikaa University, Yen Nghia, Ha Dong, Hanoi, Vietnam*

[3]*Hanoi Pedagogical University 2, Vinh Phuc, Vietnam*

[4]*Swinburne University of Technology, 463-477 Burwood Road, Hawthorn VIC 3122, Australia*

Received 16 March 2023
Revised 17 May 2023; Accepted 25 May 2023

Abstract: Calcium titanate ($CaTiO_3$), a multi-metal oxide has received extensive attention in recent years, due to its unique structural features, high chemical stability, strong catalytic activity, inexpensiveness, low toxicity, and easy synthesis. In this work, we have focused our research on and investigated the influence of Ca weight on the microstructure and properties of $CaTiO_3$ films. $CaTiO_3$ films on TiO_2 nanotube templates were synthesized using hydrothermal method at 200 ^oC for 24 h. The TiO_2 template was synthesized by anodizing using a Ti plate. The synthesized materials were analyzed on their crystal phase, surface morphology, Raman characterization, surface roughness, and hydrophilic properties by X-ray diffraction (XRD), Raman, scanning electron microscopy (SEM), 3D optical Profilometer, and contact angle measurement. The synthesized film exhibited a morphological transformation from nanotube morphology to nanopillars. Notably, the hydrophilic properties and the surface roughness of the $CaTiO_3$ films were altered after hydrothermal treatment of the TiO_2 nanotube template. These findings could potentially lead to the development of highly efficient materials for use in biomedical implants.

Keywords: $CaTiO_3$, hydrothermal, titanium, hydrophilic, surface roughness.

* Corresponding author.
E-mail address: vuong.phamhung@hust.edu.vn

https//doi.org/10.25073/2588-1124/vnumap.4841

1. Introduction

Calcium titanate ($CaTiO_3$) was discovered for the first time in 1839 by Gustav Rose, a German mineralogist. $CaTiO_3$ is a ceramic material that has been widely used in electronic devices. $CaTiO_3$ belongs to the group of materials with a perovskite-type structure. Currently, various wet chemical methods have been used to synthesize $CaTiO_3$ materials, including sol–gel [1-3], co-precipitation [4], combustion [5], organic–inorganic solution technique, and hydrothermal method [6]. Among these methods, the hydrothermal method has received significant attention due to its simple preparation technique.

As a multifunctional material, perovskite $CaTiO_3$ exhibits remarkable properties, including optical properties, high dielectric constant, ferroelectricity, chemical stability, modest dielectric loss, low cost, and eco-friendly nature [7]. Given its diverse and vast applications, various properties of $CaTiO_3$ have been extensively studied for its use in various fields. It has been extensively researched as electro-ceramic material, due to its electrical properties, which are applied in electronic devices such as capacitors and thermistors [8, 9]. $CaTiO_3$ has also been investigated for its dynamic efficiency and capacity for photocatalytic activity in degrading organic dye waste in aqueous environments and water splitting for H_2 production, and CO_2 reduction [10-12]. Furthermore, $CaTiO_3$ has been developed as an implant material in combination with hydroxyapatite for biomedical applications [13-15]. Additionally, $CaTiO_3$ possesses other advantages, such as low cost, facile synthesis, and high stability, resistance to photo corrosion.

Titanium (Ti) is considered as a fundamental material for orthopedic surgeries in heavy load conditions. However, Ti has relatively poor bone-forming properties. To overcome the disadvantages arising from the slow reaction rate in bone formation between implants and bone tissues, it is necessary to enhance osteoconductivity by applying bioactive coatings on implants. Various nano bio-coatings have been investigated to improve bioactivity using coating materials such as TiO_2 and hydroxyapatite. It has been reported that $CaTiO_3$ proposed bioactivity, and as a result, many surface modifications have been proposed to synthesize $CaTiO_3$ coatings on Ti substrates. The $CaTiO_3$ coatings have been found to significantly accelerate apatite nucleation on Ti substrates [16].

In this work, we investigated the influence of Ca content on the conversion, structural morphology properties, and properties of $CaTiO_3$ films synthesized by hydrothermal method using TiO_2 nanotube templates. Moreover, we showed the difference in the surface roughness and hydrophilic between of $CaTiO_3$ films, TiO_2 nanotubes, and Ti substrate for potential use in biomedical implants.

2. Experimental

2.1. Synthesis of $CaTiO_3$ Films

$CaTiO_3$ was synthesized using a hydrothermal process on the TiO_2 nanotube template, the mass of Ca element (x) was chosen as x = 4, 5, 6 and 7.4 mg. The TiO_2 nanotube template was grown on a Ti plate using an anodizing method at 50 V for 1 h. The initial materials for the synthesis of $CaTiO_3$ were TiO_2 nanotube template, calcium hydroxide $Ca(OH)_2$ (99.9% purity, Merck) and natri hydroxide NaOH (≥ 97.0% purity, Merck). Initially, a stoichiometric amount of $Ca(OH)_2$ was dissolved in 40 mL of H_2O, and NaOH was dissolved in 10 mL of H_2O, two mixtures were kept under stirring at room temperature for 15 min. Afterward, the two mixtures were mixed and stirred magnetically for 1 h. The resulting mixture was sealed in a 100 mL Teflon-lined stainless steel autoclave containing the TiO_2 nanotube template and then heated at 200 ºC for 24 h. After the hydrothermal process, the samples were collected, washed with deionized water (three times) and absolute ethanol (two times), and dried at 60 ºC for 12 h.

2.2. Characterization

The crystalline structure of the synthesized samples were characterized using an X-ray powder diffractometer (Siemens D500, using Cu-K_α radiation at λ = 1.5406 Å; tube voltage = 40 kV; tube current = 40 mA). The scanning diffraction angles range from 2θ = 20-80º with a scanning rate of 6.0 º/min Scanning Electron Microscopy (SEM, JSM-7600F, JEOL) was used to assess the influence of the morphology of the samples. Micro-Raman scattering (μRS) measurements were recorded using a Raman Renishaw instrument (United Kingdom). The elemental analysis was performed using the energy diperive X-ray detector (EDS, Gatan, UK) technique coupled to the FESEM. A 3D optical Profilometer system was used for the characterization of the films. The super hydrophobicity property was assessed by determining the contact angle between a water droplet and the underlying surface.

3. Results and Discussion

3.1. The Surface Morphology and Structure of $CaTiO_3$ Films

Figure 1 shows the XRD patterns of the $CaTiO_3$ films synthesized by the hydrothermal method with different Ca mass. The crystalline phase of $CaTiO_3$ was confirmed by comparing the XRD patterns of the $CaTiO_3$ films with the respective Inorganic Crystal Structure Database (ICDS) No. 06-2149. All diffraction peaks were assigned to the cubic structure of $CaTiO_3$ films with space group $Pm\bar{3}m$. Additionally, a diffraction peak of the TiO_2 phase was observed, this is due to the use of TiO_2 as the template. The intensity of the TiO_2 phase decreased as the mass of Ca increased. These results indicated that the hydrothermal conversion of $CaTiO_3$ films from the TiO_2 template is Ca mass dependent and that 7.4 mg of Ca is the most effective conversion for $CaTiO_3$ films.

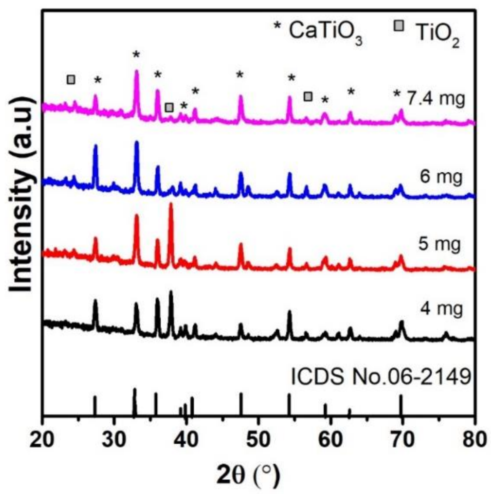

Figure 1. XRD patterns of $CaTiO_3$ films synthesis by hydrothermal method with different Ca weight.

Figure 2a shows the surface morphology of the TiO_2 nanotube template on the Ti plate, synthesized by anodizing at 50 V for 1 hour. As shown in Figure 2a, highly ordered TiO_2 nanotubes with an overall diameter of 10 nm were observed, as shown in Figure 2a. Figure 2b shows a representative of $CaTiO_3$ films on the TiO_2 nanotube template synthesized by the hydrothermal method using 7.4 mg of Ca. Instead of nanotubular morphology, the hydrothermal treatment of the TiO_2 nanotube template led to the formation of a nanopillar structure conversion.

The morphology of the $CaTiO_3$ film was examined more by tilting the direction of the $CaTiO_3$ film observation, as shown in Figure 2c. The nanopillar structure of the $CaTiO_3$ film confirmed that the structure was formed from a TiO_2 nanotube template and the thickness of the $CaTiO_3$ layer of 200-300 nm. These results indicated that hydrothermal treatment of the TiO_2 nanotube template can induce significant changes in the structures of the $CaTiO_3$ films.

Figure 2d shows the EDS spectra of the $CaTiO_3$ film sample. The spectra reveal clear signals of oxygen, calcium, titanium, erbium, and sodium elements in the samples. The presence of sodium element in the sample is likely due to residual input solution. According to previous studies, the element Na does not affect the formation of $CaTiO_3$ film coating on the Ti [17-19]. When treating titanium samples with NaOH solution will increase the biocompatibility of the material.

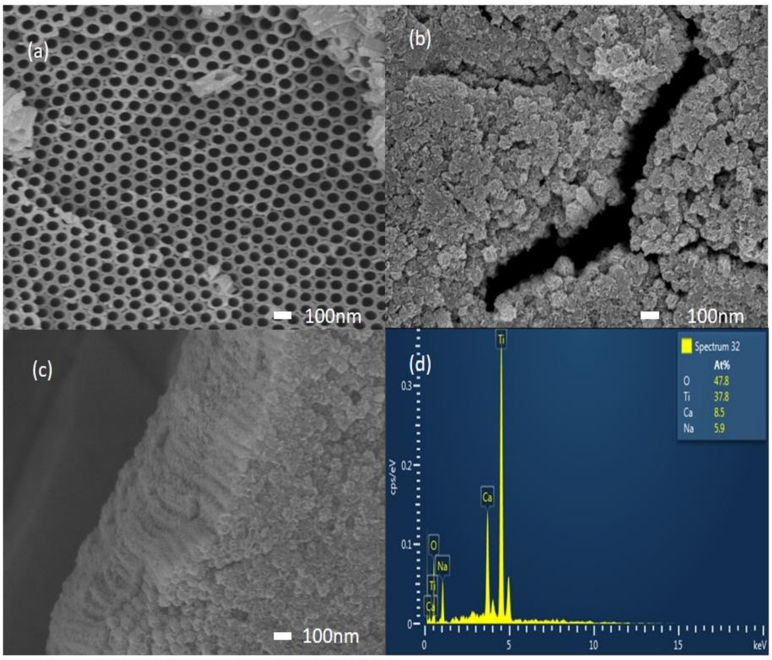

Figure 2. Surface morphology of TiO_2 nanotube template (a), $CaTiO_3$ film on TiO_2 nanotubes template (b), $CaTiO_3$ film with tilt the observation direction (c), and EDS spectra of $CaTiO_3$ film (d).

According to the orthorhombic structure *Pbnm* (Z^B= 4) of $CaTiO_3$, there are a total of 24 Raman-active modes, with four molecular units in the primitive cell and an irreducible representation of $\Gamma_{\text{Raman},\ Pbnm} = 7A_g+5B_{1g}+7B_{2g}+5B_{3g}$ [20-21]. Figure 3 shows the Raman spectra of $CaTiO_3$ in the frequency range of 100–900 cm^{-1}. Raman active modes that are commonly observed include: 134 cm^{-1} for a vibration of Ca bonded to a TiO_3 group (Ca–TiO_3) lattice mode; 226, 244, 281, and 362 cm^{-1} are associated with O–Ti–O bending modes; 464 and 495 cm^{-1} correspond to Ti–O_6 torsional (bending or internal vibration of the oxygen cage) modes, and a second broad band at 600–700 cm^{-1}. These results are consistent with the previous works [21-25].

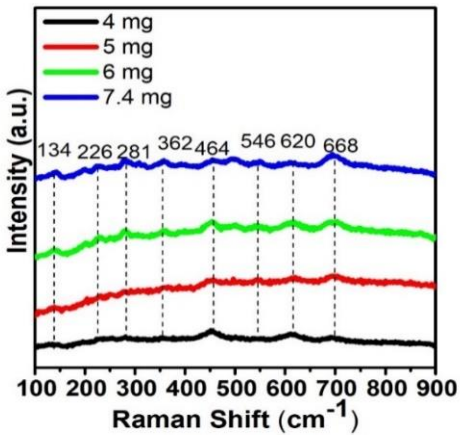

Figure 3. Raman spectra of $CaTiO_3$ film corresponding to the different Ca mass.

3.2. Material Surface Morphology

Figure 4 shows the 3D optical profilometry results of the Ti substrate, TiO_2 nanotubes, and $CaTiO_3$ films. The average (R_a) surface roughness was lowest for the Ti substrate, while it was highest for the $CaTiO_3$ films. Specifically, the surface roughness of the Ti, TiO_2, and $CaTiO_3$ films was measured at 0.35 µm, 0.60 µm, and 1.86 µm, respectively, as shown in Figure 5. These results suggest that the hydrothermal synthesis of $CaTiO_3$ films using TiO_2 nanotube templates increased the surface roughness.

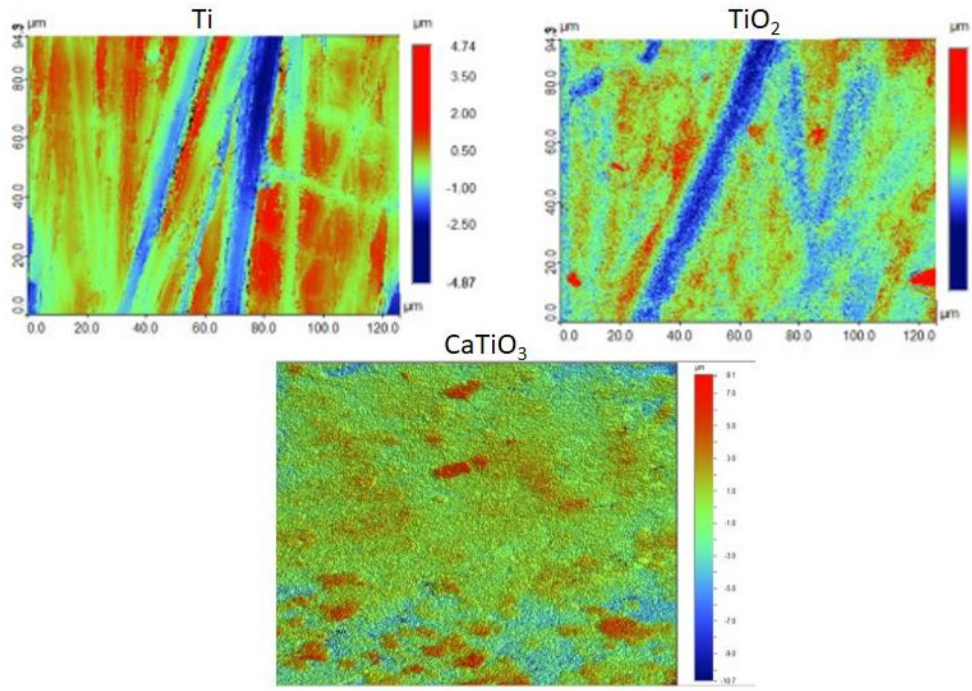

Figure 4. 3D optical Profilometer topographic of Ti substrate, TiO_2 nanotubes, and $CaTiO_3$ films.

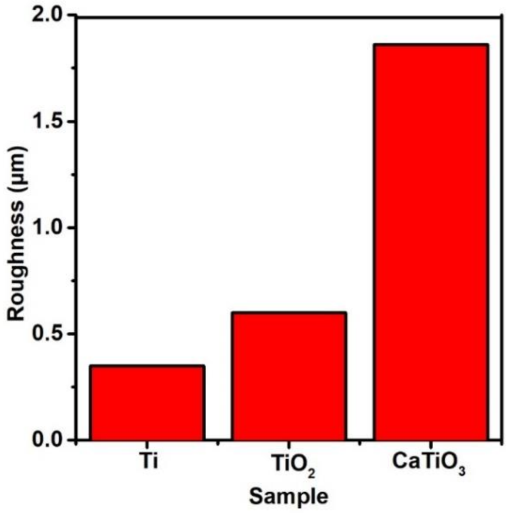

Figure 5. Graph of the surface roughness of the Ti substrate, TiO_2 nanotubes, and $CaTiO_3$ films

Contact angle measurements using deionized water revealed a significantly lower contact angle for the $CaTiO_3$ surface compared to the untreated Ti and TiO_2 nanotubes (Fig. 6). This indicates that the $CaTiO_3$ films have superior surface hydrophilicity. Notably, there were significant differences in contact angles between the Ti, TiO_2, and $CaTiO_3$ films. The water contact angles of the Ti, TiO_2, and $CaTiO_3$ films were found to be 43°, 24°, and 2°, respectively. Previous studies have shown that $CaTiO_3$ film has a more positive charge in aqueous solution than anatase due to the point of zero charge high (PZC) of $CaTiO_3$, which is much more than that of anatase [26]. Therefore, the topography-dependent wettability effect of the submicron-structured Ca samples could be offset by the high PZC of the $CaTiO_3$ structure. It has also been reported that thermal oxidation decreases the PZC of Ti alloy, and the creation of nanoscale surface porosity by thermal treatment can increase surface wettability [27]. Thus, in conjunction with the formation of anatase structure in the Ca-incorporated film, which is believed to carry a negative surface charge in aqueous solution, the increased surface area at the nano-scale appears to considerably decreased contact angles on the $CaTiO_3$ surface.

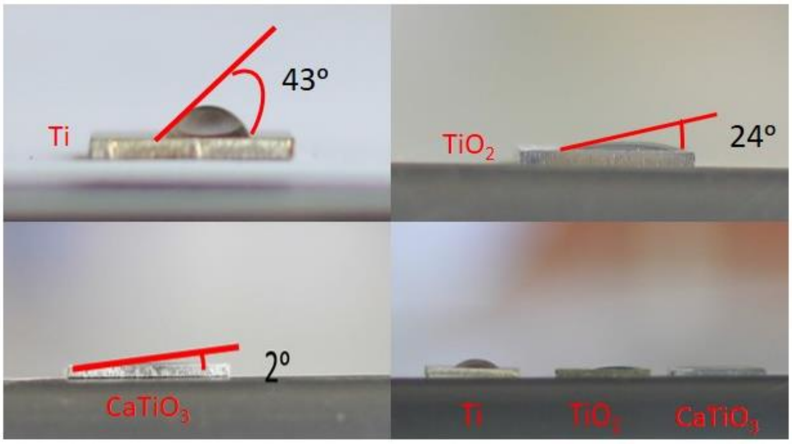

Figure 6. The water contact angles of Ti, TiO_2, and $CaTiO_3$ films.

4. Conclusion

In this work, the $CaTiO_3$ nanotube films were synthesized on a TiO_2 nanotube template through a hydrothermal treatment process at 200 °C for 24 h. The $CaTiO_3$ films inherited the nanopillar structures of the TiO_2 nanotubes. The $CaTiO_3$ films exhibited superior hydrophilic surface characteristics. The water contact angle of the $CaTiO_3$ films were found to be 2°. Besides, it was observed that the surface roughness of the $CaTiO_3$ film was significantly higher than that of the Ti substrate and TiO_2 nanotubes. The surface roughness of the $CaTiO_3$ films gains a value of 1.86 µm. With the above advantages, $CaTiO_3$ films meet the requirements of current biomedical applications, typically titanium implants.

Acknowledgments

This research was funded by the Ministry of Education and Training (MOET) under grant number CT2022.03.BKA.01

References

[1] G. Pfaff, Synthesis of Calcium Titanate Powders by the Sol-Gel Process, Chem. Mater, Vol. 6, 1994, pp. 58-62, https//doi.org/10.1021/cm00037a013.

[2] M. Manso, M. Langlet, J. M. M. Duart, Testing Sol-gel $CaTiO_3$ Coatings for Biocompatible Applications, Mater. Sci. Eng. C, Vol. 23, 2003, pp. 447-450, https//doi.org/10.1016/S0928-4931(02)00319-3.

[3] S. Holliday, A. Stanishevsky, Crystallization of $CaTiO_3$ by Sol-gel Synthesis and Rapid Thermal Processing, Surf. Coatings Technol, Vol. 188-189, 2004, pp. 741-744, https//doi.org/10.1016/j.surfcoat.2004.07.044.

[4] X. Zhang, J. Zhang, X. Ren, X. J. Wang, The Dependence of Persistent Phosphorescence on Annealing Temperatures in $CaTiO_3$:Pr^{3+} Nanoparticles Prepared by A Coprecipitation Technique, J. Solid State Chem, Vol. 181, 2008, pp. 393-398, https//doi.org/10.1016/j.jssc.2007.11.022.

[5] M. Muthuraman, K. C. Patil, S. Senbagaraman, A. M. Umarji, Sintering, Microstructural and Dilatometric Studies of Combustion Synthesized Synroc Phases, Mater. Res. Bull, Vol. 31, 1996, pp. 1375-1381, https//doi.org/10.1016/0025-5408(96)00131-6.

[6] T. R. N. Kutty, R. Vivekanandan, P. Murugaraj, Precipitation of Rutile and Anatase (TiO_2) Fine Powders and their Conversion to $MTiO_3$ (M = Ba, Sr, Ca) by the Hydrothermal Method, Mater. Chem. Phys, Vol. 19, 1988, pp. 533-546, https//doi.org/10.1016/0254-0584(88)90045-4.

[7] C. Karthikeyan, M. Thamima, S. Karuppuchamy, Structural and Photocatalytic Property of $CaTiO_3$ Nanosphere, Mater. Sci. Foru, Vol. 979, 2020, 169-174, https//doi.org/10.4028/www.scientific.net/MSF.979.169.

[8] C. L. Huang, C. L. Pan, S. J. Shium, Liquid Phase Sintering of $MgTiO_3$-$CaTiO_3$ Microwave Dielectric Ceramics, Mater. Chem. Phys, Vol. 78, 2003, pp. 111-115, https//doi.org/10.1016/S0254-0584(02)00311-5.

[9] J. Li, Y. Wang, X. Yang, H. Kang, Z. Cao, X. Jiang, Z. Chen, E. Guo, T. Wang, Processing Bulk Insulating $CaTiO_3$ into A High-performance Thermoelectric Material, Chem. Eng. J, Vol. 428, 2022, pp. 131121, https//doi.org/10.1016/j.cej.2021.131121.

[10] Y. Yan, H. Yang, X. Zhao, R. Li, X. Wang, Enhanced Photocatalytic Activity of Surface Disorder-engineered $CaTiO_3$, Mater. Res. Bull, Vol. 105, 2018, pp. 286-290, https//doi.org/10.1016/j.materresbull.2018.05.008.

[11] T. Soltani, X. Zhu, A. Yamamoto, S. P. Singh, E. Fudo, A. Tanaka, H. Kominami, H. Yoshida, Effect of Transition Metal Oxide Cocatalyst on the Photocatalytic Activity of Ag loaded $CaTiO_3$ for CO_2 Reduction with Water and Water Splitting, Appl. Catal. B Environ, Vol. 286, 2021, pp. 119899, https//doi.org/10.1016/j.apcatb.2021.119899.

[12] H. Chouirfa, H. Bouloussa, V. Migonney, C. F. Daudré, Review of Titanium Surface Modification Techniques and Coatings for Antibacterial Applications, Acta Biomater, Vol. 83, 2019, pp. 37-54, https//doi.org/10.1016/j.actbio.2018.10.036.

[13] A. K. Dubey, B. Basu, K. Balani, R. Guo, A. S. Bhalla, Multifunctionality of Perovskites $BaTiO_3$ and $CaTiO_3$ in A Composite with Hydroxyapatite as Orthopedic Implant Materials, Integr. Ferroelectr, Vol. 131, 2011, pp. 119-126, https//doi.org/10.1080/10584587.2011.616425.

[14] M. Li, M. J. Mondrinos, X. Chen, M. R. Gandhi, F. K. Ko, P. I. Lelkes, Elastin Blends for Tissue Engineering Scaffolds, J. Biomed. Mater. Res. Part A, Vol. 79, 2006, pp. 963-973, https//doi.org/10.1002/jbm.a.

[15] G. Gralik, C. Zanelli, F. R. Pereira, M. Dondi, J. A. Labrincha, D. Hotza, Formation and Quantification of Calcium Titanate with the Perovskite Structure from Alternative Sources of Titanium, 21 CBECIMAT - Congr. Bras. Eng. E Ciência Dos Mater, 09 a 13 Novembro 2014, Cuiabá, MT, Bras. 2014, pp. 503-510, Available: http://www.metallum.com.br/21cbecimat/CD/PDF/104-016.pdf (accessed on: February 8th, 2023).

[16] J. Wei, T. Igarashi, N. Okumori, T. Igarashi, T. Maetani, B. Liu, M. Yoshinari, Influence of Surface Wettability on Competitive Protein Adsorption and Initial Attachment of Osteoblasts, Biomed. Mate., Vol. 4, 2009, pp. 045002, https//doi.org/10.1088/1748-6041/4/4/045002.

[17] S. Ban, Effect of Alkaline Treatment of Pure Titanium and Its Alloys on the Bonding Strength of Dental Veneering Resins, J. Biomed. Mater. Res. - Part A, Vol. 66, 2003, pp. 138-145, https//doi.org/10.1002/jbm.a.10566.

[18] F. Hamzah, Surface Characterization on Alkali-Heat-Treatment on Titanium Alloy, Malaysian J. Anal. Sci, Vol. 20, 2016, pp. 1429-1436, https//doi.org/10.17576/mjas-2016-2006-23.

[19] D. L. Morgan, Alkaline Hydrothermal Treatment of Titanate, PhD Thesis, Queensland University of Technology, 2010.

[20] Y. Li, S. Qin, F. Seifert, Phase Transitions in A-site Substituted Perovskite Compounds: The $(Ca_{1-2x}Na_xLa_x)TiO_3$ $(0 \leq x \leq 0.5)$ Solid Solution, J. Solid State Chem, Vol. 180, 2007, pp. 824-833, https//doi.org/10.1016/j.jssc.2006.12.012.

[21] M. L. Moreira, E. C. Paris, G. S. D. Nascimento, V. M. Longo, J. R. Sambrano, V. R. Mastelaro, M. I. B. Bernardi, J. Andrés, J. A. Varela, E. Longo, Structural and Optical Properties of $Catio_3$ Perovskite-based Materials Obtained by Microwave-assisted Hydrothermal Synthesis: An Experimental and Theoretical Insight, Acta Mater, Vol. 57, 2009, pp. 5174-5185, https//doi.org/10.1016/j.actamat.2009.07.019.

[22] H. Zheng, I. M. Reaney, G. D. C. C. D. Györgyfalva, R. Ubic, J. Yarwood, M. P. Seabra, V. M. Ferreira, Raman Spectroscopy of $CaTiO_3$-based Perovskite Solid Solutions, J. Mater. Res, Vol. 19, 2004, pp. 488-495, https//doi.org/10.1557/jmr.2004.0059.

[23] P. McMillan, N. Ross, The Raman Spectra of Several Orthorhombic Calcium Oxide Perovskites, Phys. Chem. Miner, Vol. 16, 1988, pp. 21-28, https//doi.org/10.1007/BF00201326.

[24] S. Qin, X. Wu, F. Seifert, A. I. Becerro, Micro-Raman Study of Perovskites in the $CaTiO_3$-$SrTiO_3$ System, J. Chem. Soc. Dalt. Trans., Vol. 2002, pp. 3751-3755, https//doi.org/10.1039/b207228a.

[25] P. Gillet, F. Guyot, G. D. Price, B. Tournerie, A. Le Cleach, Phase Changes and Thermodynamic Properties pf $Catio_3$, Spectroscopic Data, Vibrational Modelling and Some Insights on the Properties of $MgSiO_3$ Perovskite, Phys. Chem. Miner, Vol. 20, 1993, pp. 159-170, https//doi.org/10.1007/BF00200118.

[26] D. E. M. Donald, B. E. Rapuano, H. C. Schniepp, Surface Oxide Net Charge of A Titanium Alloy: Comparison Between Effects of Treatment with Heat or Radiofrequency Plasma Glow Discharge, Colloids Surfaces B Biointerfaces, Vol. 82, 2011, pp. 173-181, https//doi.org/10.1016/j.colsurfb.2010.08.031.

[27] M. Passi, B. Pal, A Review on $Catio_3$ Photocatalyst: Activity Enhancement Methods and Photocatalytic Applications, Powder Technol, Vol. 388, 2021, pp. 274-304, https//doi.org/10.1016/j.powtec.2021.04.056.